Investigation of Electrical Means of Dust Removal From Solar Panels For Martian Applications

Rishita Mhatre* and Viti Chandra†
Georgia Institute of Technology, Atlanta, Georgia, 30332

As evidenced by agencies such as NASA, the future of autonomous and manned space exploration and eventual sustained human presence relies on the development of key infrastructure and energy capabilities. When considering the Martian environment, solar panels have historically been utilized for energy generation. However, a key obstacle in their widespread use has been the effect of Martian dust coating solar panels and hindering energy generation. Many flagship missions such as NASA's Opportunity rover saw the end of their missions as a result of being unable to continue collecting solar energy. Current practices to mitigate this issue have largely been mechanical or operational and still lack overall effectiveness due to electrically charged dust being more difficult to remove with these methods. Thus, this team decided to pursue an investigation into electrical methods of clearing dust from solar panels and understand its future applicability. After validating the use of a controlled sweep of a charged electrode across an ITO-coated glass, the experiment was extended to measure the dust removal efficiency of four electrode materials (aluminum, copper, sterling silver, and nickel) across single and triple passes. Of these tests, aluminum demonstrated the highest dust removal efficiency with lowest variability.

I. Introduction

Previously, the team initiated a proof of concept in which the method of using an electrode for dust removal was substantiated. The team designed a unique setup to pass an electrode over a ITO-coated glass panel, and studied the percentage of simulated regolith removed via Matlab image processing. The initial experiment led to findings that the electrode was able to pick up regolith particles from the glass panel. However, the efficiency of this method decreased as the average dust particle size also decreased. In other words, finer particles tended to be stickier, and hence were more difficult to remove. Thus, this initial proof of concept validated the method but offered areas for further investigation and hence is the topic of this paper. Following the initial results, the team decided to explore the efficacy of the electrode material on the removal of the regolith, as an effort to solve the issues seen in the prior iteration. With the team's goal of finding an electrode material that will increase the efficacy of the method, the team selected four electrode materials to test. This research aims to provide additional evidence for the electrode method while also offering ways for further extending its viability.

*Undergraduate Student, Department of Aerospace Engineering, Atlanta, GA, AIAA Student Member 1537138
†Undergraduate Student, Department of Aerospace Engineering, Atlanta, GA, AIAA Student Member 1931462

II. Problem and Objective

The Electrostatics and Surface Physics Laboratory at NASA's Kennedy Space Center developed the Electrodynamic Dust Shield (EDS), a dust mitigation technology that operates by producing time-varying, non-uniform electric fields capable of mobilizing electrically charged dust particles. The system employs a dielectric surface embedded with a fine electrode grid driven by a low-power, multiphase AC signal. This configuration generates a traveling electric field across the surface, causing charged dust particles to move as a result of Coulomb and dielectrophoretic forces created by the field's spatial non-uniformity.

Building on a similar principle, the MIT Energy Initiative investigated an approach aimed at reducing water consumption for cleaning solar panels in terrestrial solar farms and power plants. In research led by MIT graduate student Sreedath Panat and mechanical engineering professor Kripa Varanasi, the team designed a system in which an electrode traverses the surface of a solar panel coated with a transparent conductive layer. As the electrode moves, it generates an electric field that induces charge on dust particles. By determining an appropriate voltage range, the researchers identified conditions under which gravitational and adhesive forces could be overcome, allowing the dust to detach from the panel surface. This experimental framework later informed early design concepts for extending the technique to remove Martian regolith from solar panels.

It is important to distinguish that the MIT Energy Initiative's experiments were conducted under Earth-based conditions and primarily targeted solar panel maintenance in terrestrial environments. Results showed that ambient humidity played a significant role, as moisture in the air formed a thin water layer on dust particles, enabling effective removal at relative humidity levels above approximately 30 percent. Although daytime humidity on Mars is extremely low—often below 0.03 percent—nighttime humidity can rise to between 80 and 100 percent. This suggests that dust removal operations could be feasible during Martian nights if appropriately scheduled. Furthermore, the experiments focused on dust and sediment types commonly found on Earth, rather than strictly Martian analog materials.

In previous experiments, the team successfully demonstrated the ability of electric fields generated by copper fiberglass electrodes to remove dust particles from solar panel surfaces. However, several challenges were identified that limited the reliability and practicality of this method. In particular, the inconsistency of the experimental setup raised concerns about the replicability of the results, as maintaining a uniform distance between the electrode and the glass panel during manual sweeps proved difficult. Furthermore, measurements were based on qualitative observations by the naked eye, leaving room for subjectivity and imprecision in assessing the amount of dust removed.

Recognizing these limitations, this study focused on improving both the precision and replicability of the previous experimental setup. Specifically, the team sought to design a rail system capable of maintaining a consistent, modifiable distance between the electrode and the glass panel during sweeps, thereby limiting a source of human error. In addition, a quantitative method for measuring dust removal was developed by creating an image processor to analyze before-and-after images of the glass panels. These refinements allowed the team to test the research question of which electrode material is the most effective at maximizing dust removal from a conductive glass panel, and whether increasing the number of passes would result in a more thorough cleaning. The team posits that sterling silver, with its high conductivity, will remove the most dust from a glass panel, and that additional passes will only marginally improve field effectiveness, as dust accumulation on the electrode reduces its efficiency over time. By systematically varying the electrode material while keeping other variables constant, the team strove to identify the optimal material and configuration for efficient dust mitigation.

III. Experimental Setup

The experimental setup for the later material dependency iteration was as follows. The team, having realized the importance of implementing reliability and replicability into the experiment design, designed a "rail-system" to hold and guide all stationary and moving aspects of the experiment. By doing so, the team sought to eliminate human intervention as much as possible, to therefore eliminate a large source of error in the data obtained. Thus, the "rail-system", features a 3D printed frame to hold the electrode, a top frame to insert the regolith filter, and a bottom slotted base to hold the glass panel. The entire system is pictured in figure 2. The rail-system also features multiple holes in the four legs supporting the system. These holes allow for the distance between the electrode and the glass panel to be changed, allowing for the team to also understand the impact of distance on the amount of dust removed as well as maintain a fixed distance above the panel.

In terms of the actual experimental procedure, a series of strings were attached to the electrode to allow for it to be moved back and forth in the slot, as the glass panel was positioned directly below. The circuit used during the experiment is shown in figure 3. The circuit setup featured a breadboard, a 15kV power supply, and alligator clips to facilitate necessary connections. Addressing the electrical setup, it can be seen that the electrode is connected to the power supply via copper tape, while the glass panel is grounded to maintain the necessary potential difference that allows for the dust removal.

In terms of the setup for the image processing portion of the experiment, the setup of the experiment also featured an LED housed in the bottom slot. The significance of this light source is to allow for the glass panel to be backlit and hence make the image processing much easier. Additional information on the data processing portion of this research can be found in the later section titled "Data Reduction".

A. Experimental Procedure

The regolith was first filtered to a uniform 600 μm particle size onto the treated glass panel. The glass panel was placed in the apparatus, slotted above the light source. An initial picture was taken immediately after setup before the start of the experiment to look at the initial percent dust coverage over the panel. The circuit components were set up as ground was attached to the glass panel and the positive voltage was attached to the electrode. The power source was turned on and the output voltage was adjusted to 24V. The electrode plate was swept through the frame over the glass panel for the predetermined number of sweeps, after which the power source was switched off and a second picture was taken of the glass panel after the experiment. The panel was wiped down with a microfiber towel after each test case. The procedure was repeated for additional material types as well as incremented number of sweeps.

B. Data Reduction

Once data had been collected from several trials, it was reduced and presented as follows. To collect data from each trial, pictures of the glass panel before and after each trial were taken via a high resolution camera. Then a Matlab script was developed, by two of the team members, which took the pictures obtained as inputs and was able to calculate the percent dust removal. This was done by analyzing the area of the image compromising the regolith before vs. after the trial. Sample images of the pictures utilized in the data reduction process are shown in figure 4. The specific formula used in the MATLAB script is detailed below.

$$\% \text{ Efficiency} = \frac{\text{Initial Coverage } \% - \text{Final Coverage } \%}{\text{Initial Coverage } \%} \times 100 \tag{1}$$

IV. Results

The experiment measured the dust removal efficiency of four electrode materials (aluminum, copper, sterling silver, and nickel) across single and triple passes.

The results, summarized in Table 7 by averaging data from Tables 4-6, revealed distinct performance trends for each material, providing insight into their suitability for practical dust mitigation applications. Efficiency percentages and standard deviations were recorded to evaluate the effectiveness and consistency of each material under identical experimental conditions, results which are visualized in Figure 5. The efficiency percentage was calculated using the aforementioned formula and the raw area percentage data presented in Tables 1-3 to eliminate the effects of varying initial amounts of dust on the panel.

Aluminum demonstrated the highest dust removal efficiency among the materials tested. With three passes, aluminum achieved an efficiency of 63.37% ± 6.83, showing a significant improvement from its single-pass performance of 56.55% ± 12.48. Its consistent results, as reflected by relatively low standard deviations, highlight its reliability and suitability for practical applications. This performance is likely attributed to aluminum's favorable material properties, which may enhance dust removal while minimizing issues such as arcing or dust adhesion to the electrode surface. These findings position aluminum as the most promising candidate for efficient and reliable dust mitigation systems. In contrast, copper exhibited the lowest dust removal efficiency. Its performance declined slightly between single and triple passes, with efficiencies of 38.80% ± 13.99 and 36.59% ± 11.9, respectively. This decrease suggests that significant dust accumulation on the electrode surface during operation impaired its performance. Copper's inability to self-clean effectively and its higher variability, as indicated by the standard deviations, highlight challenges in using this material for sustained dust removal. These limitations suggest that copper may not be a suitable choice for applications requiring consistent and high-efficiency dust mitigation.

Nickel showed moderate dust removal efficiency, with minimal variation between one pass (54.02% ± 12.59) and three passes (54.07% ± 10.48). This consistency indicates that nickel's performance does not significantly improve with additional electrode sweeps, implying diminishing returns for multiple passes. While nickel's moderate efficiency and stable performance make it a potential candidate, its lack of significant improvement with additional passes limits its utility in applications where high dust removal efficiency is critical.

Sterling silver also displayed relatively stable efficiency between single and triple passes, achieving 54.87% ± 9.39 and 47.86% ± 14.92, respectively. However, its high variability, as indicated by the larger standard deviations, suggests less predictable performance compared to the other materials. This inconsistency, combined with its lower efficiency relative to aluminum, reduces its practicality for dust mitigation systems. Additionally, sterling silver experienced significant dust accumulation on the electrode surface, further impairing its effectiveness over time. All numerical results have been tabulated in tables 1 through 7 for reference.

Several key observations were made during the experiment. First, a substantial proportion of the dust was removed immediately upon voltage application, regardless of the electrode material, highlighting the potential of electric fields for rapid initial dust mitigation. However, the effectiveness of the electrodes declined as dust accumulated on their surfaces. This was particularly evident for copper and sterling silver, which lacked self-cleaning properties, leading to a reduction in performance during subsequent passes. Furthermore, while aluminum benefited from multiple passes, other materials, such as nickel and sterling silver, showed little to no improvement, indicating diminishing returns with increased sweeps.

Finally, we observed that the thickness of the dust layer significantly influenced cleaning effectiveness, with thicker layers reducing efficiency across all electrode materials due to the electric field's difficulty in dislodging cohesive dust. Panels with lighter initial dust coverage appeared cleaner after trials, even with similar efficiency percentages, highlighting the importance of initial dust conditions in achieving optimal and uniform cleaning. The findings of this experiment have significant implications for the design of dust mitigation systems in dusty environments, such as on Mars rovers.

Aluminum emerged as the most efficient and reliable electrode material due to its high dust removal capability, low variability, and improvement with multiple passes. However, the diminishing returns observed with increased passes suggest that optimizing the number of sweeps and incorporating mechanisms to clean the electrode surface during operation could further enhance performance.

These results underscore the importance of selecting materials with favorable properties and designing systems that maximize operational efficiency and reliability while minimizing costs and complexity.

V. Challenges, Iterations, & Sources of Error

The team faced a variety of challenges throughout the implementation of this research project. Incorporating motors into the apparatus posed the largest obstacle as inconsistent performance, sizing issues, and time constraints led to the decision to manually sweep the electrode for the current experiment. Automation remains a priority for future iterations, and early integration of more advanced and reliable motor models will enable precise and consistent operation.

Another critical challenge involved quantifying results, which was addressed using MATLAB's image processing software. This approach provided a systematic method to analyze experimental outcomes, ensuring consistency and replicability. Moving forward, automating this process alongside motorized sweeping will further streamline experimentation. These iterations and challenges reflect the evolving nature of the design process, emphasizing the need for flexibility, precise tolerancing, and early integration of key components to optimize both performance and usability.

VI. Conclusion

Aluminum emerged as the most effective electrode material, achieving the highest efficiency after three passes (63.37%) and showing significant improvement with additional sweeps. Its low cost, lightweight properties, and ability to naturally resist corrosion through a protective oxide layer make it a practical choice for large-scale applications, such as on a Martian rover. While the 1-pass trials for aluminum exhibited higher standard deviation (±12.48%), its overall performance remained reliable compared to other materials. Copper demonstrated the lowest efficiency across all trials (38.80% → 36.59%), with rapid performance degradation due to dust accumulation. Sterling silver displayed steady efficiency between one and three passes (54.87% → 54.06%), but the lack of significant improvement with additional sweeps highlighted its limited cleaning potential. Nickel showed diminished returns with more passes (54.02% → 47.86%), suggesting sensitivity to dust buildup. The results challenge our initial hypothesis favoring sterling silver, as its performance was hindered by tarnishing risks and poor adaptability to multiple sweeps. Aluminum's superior balance of properties—including conductivity, malleability, and strength-to-weight ratio—makes it well-suited for extraterrestrial applications. However, questions remain regarding potential dust adhesion effects on long-term efficiency, whether auxiliary cleaning mechanisms are required, and how this method would perform under real-world rover conditions. Further exploration, such as testing voltage pulses instead of constant voltage, could optimize the cleaning process and address dust redistribution challenges caused by elevation changes.

Future work is needed to continue to refine the experimental set-up, better simulate real-world conditions and applications, and explore the potential of non-constant electric fields. Improved performance and replicability are essential to continue testing a variety of factors. Future work will explore the potential of using a non-constant electric field, such as voltage pulses or sinusoidal patterns, to enhance dust removal. Our findings suggest that the most significant dust removal occurs when the power supply is initially activated, indicating that introducing pulsations or transitioning to an AC wave could improve efficiency by generating oscillatory forces to dislodge dust more effectively. This approach could be particularly advantageous under Martian conditions, where adhesive dust bonds present unique challenges. Testing different surfaces, such as those found on rover components, will further refine this method's applicability.

Enhancements to the experimental apparatus are also essential for improved performance and replicability. Automating the sweep mechanism with more advanced and reliable motors will address torque insufficiencies in the current motor-spool assembly. Replacing the nylon string with a thicker Kevlar string could tighten the electrode-to-motor connection, ensuring smoother horizontal movement. Automating the application of dust on the panel will allow precise control of variables such as electrode speed and dust distribution, improving experimental consistency.

To better simulate real-world applications, future iterations will incorporate Martian conditions, including temperature, pressure, and dust composition. This will help evaluate the feasibility of integrating the experimental setup with a rover while considering mass implications and structural requirements. A redesign of the apparatus to be lighter, more compact, and suitable for rover constraints will enhance its viability.

Additionally, upgrading the imaging and processing system will streamline the experiment. Replacing the current camera and LED light setup with a multi-purpose Arducam OwlSight integrated with a Raspberry Pi will reduce material requirements and ensure seamless processing between image capture and efficiency calculations. This change will make the system more compact, cost-effective, and replicable in diverse settings.

Reflecting on the limitations of our current design and incorporating these advancements, we aim to develop a more robust and efficient system that aligns with the challenges of Martian exploration and expands its potential applications.

Appendix

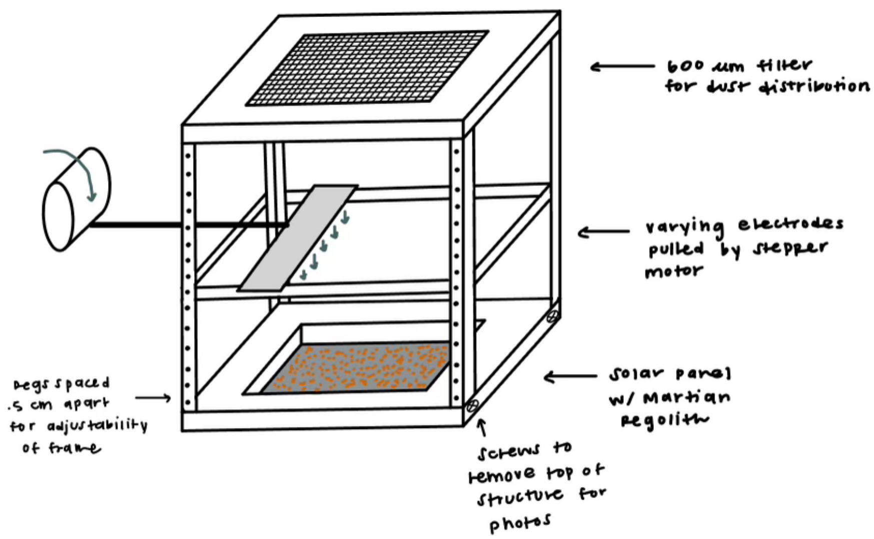

Fig. 1 Initial sketch of experimental frame design.

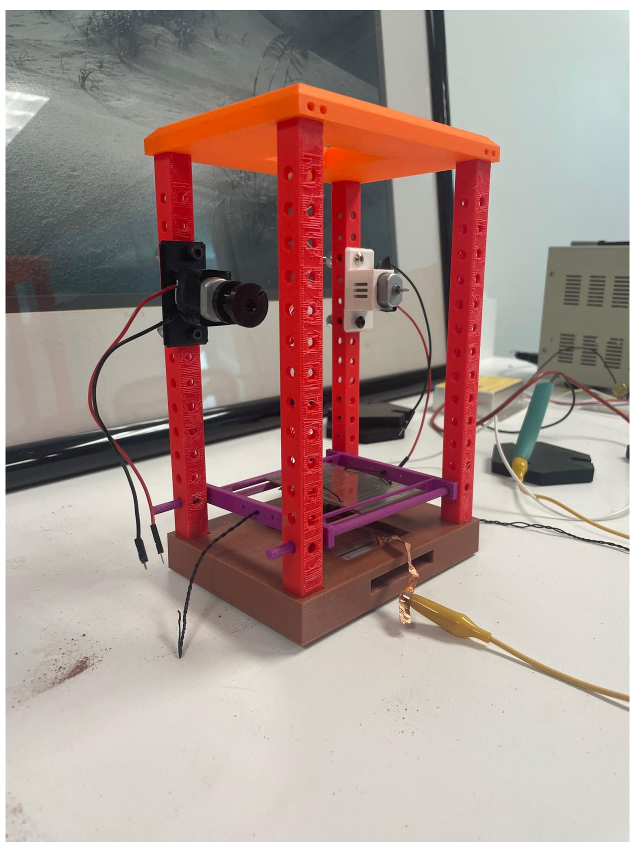

Fig. 2 Detailed view of "rail-system".

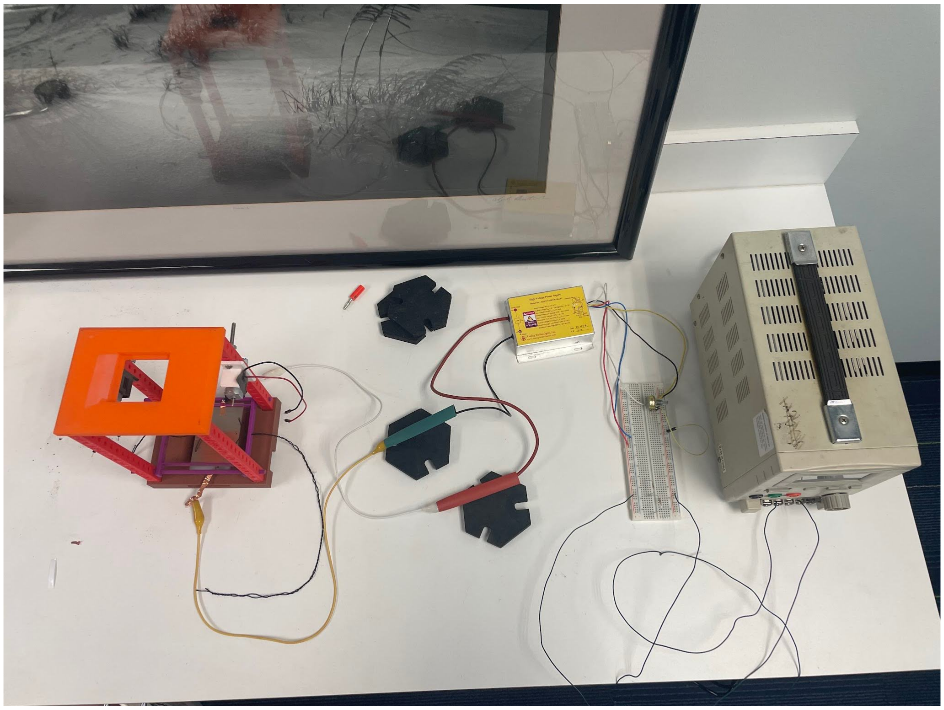

Fig. 3 Full experimental setup.

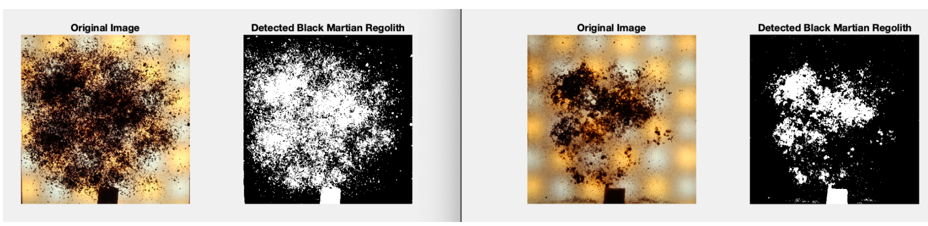

Fig. 4 "Before" and "After" Sample Images of Code Input & Output

Table 1 Trial 1 raw data for each electrode material

	3 Pass		1 Pass	
	% Before	% After	% Before	% After
Aluminum	49.53%	22.03%	43.36%	24.67%
Copper	40.48%	29.41%	40.87%	23.71%
Sterling Silver	46.62%	27.55%	37.17%	15.35%
Nickel	36.65%	17.35%	46.97%	24.59%

Table 2 Trial 2 raw data for each electrode material

	3 Pass		1 Pass	
	% Before	% After	% Before	% After
Aluminum	18.90%	6.04%	31.20%	10.06%
Copper	30.88%	20.80%	50.66%	38.76%
Sterling Silver	43.10%	26.86%	54.89%	30.65%
Nickel	44.02%	24.48%	30.76%	16.65%

Table 3 Trial 3 raw data for each electrode material

	3 Pass		1 Pass	
	% Before	% After	% Before	% After
Aluminum	40.21%	13.45%	28.69%	11.82%
Copper	36.64%	18.40%	39.68%	19.47%
Sterling Silver	35.19%	12.32%	32.03%	12.25%
Nickel	30.42%	10.59%	36.71%	11.56%

Table 4 Trial 1 % Efficiency of each electrode material with quantified observed arcing

	3 Pass		1 Pass	
	% Efficiency	Arc Count	% Efficiency	Arc Count
Aluminum	55.52%	0	43.10%	0
Copper	27.35%	0	41.99%	0
Sterling Silver	40.91%	0	58.70%	0
Nickel	52.66%	0	47.65%	0

Table 5 Trial 2 % Efficiency of each electrode material with quantified observed arcing

	3 Pass		1 Pass	
	% Efficiency	Arc Count	% Efficiency	Arc Count
Aluminum	68.04%	0	67.76%	0
Copper	32.64%	0	23.49%	0
Sterling Silver	37.68%	0	44.16%	0
Nickel	44.38%	0	45.87%	0

Table 6 Trial 3 % Efficiency of each electrode material with quantified observed arcing

	3 Pass		1 Pass	
	% Efficiency	Arc Count	% Efficiency	Arc Count
Aluminum	66.55%	0	58.80%	0
Copper	49.78%	0	50.93%	0
Sterling Silver	64.99%	0	61.75%	0
Nickel	65.19%	0	68.51%	0

Table 7 Average efficiency with standard deviation calculation for each electrode material and their respective passes

	3 Pass		1 Pass	
	% Efficiency	Standard Deviation	% Efficiency	Standard Deviation
Aluminum	63.37%	± 6.83%	56.55%	± 12.48%
Copper	36.59%	± 11.9%	38.80%	± 13.99%
Sterling Silver	47.86%	± 14.92%	54.87%	± 9.39%
Nickel	54.07%	± 10.48%	54.02%	± 12.59%

Acknowledgments

The authors of this paper would like to extend their sincerest gratitude to the rest of the M.A.R.S. VIP Dust Mitigation team at Georgia Tech and the faculty advisors for their support and participation throughout the process. The research conducted in this paper is to be attributed to their joint efforts. This group includes team members Nishita Tonangi, Cassandra Riquelme, and Yana Batra, as well as faculty Advisors, Dr. John Hankinson and Dr. Mathew Swarts.

References

[1] "Aluminium: Specifications, properties, classifications and classes," https://www.azom.com/article.aspx?ArticleID=2863, May 2005. Accessed: 2024-2-26.

[2] Conniff, M., and Zidonis, A., "Copper: Definition, composition, properties, and industrial applications," https://www.xometry.com/resources/materials/what-is-copper/, Apr. 2023. Accessed: 2024-2-26.

[3] https://www.globalspec.com/learnmore/materials_chemicals_adhesives/electrical_optical_, ???? Accessed: 2024-2-26.

[4] Gude, V. G., "Microbial Fuel Cells as a Platform Technology for Sustainable Wastewater Treatment," *Progress and Recent Trends in Microbial Fuel Cells*, Elsevier, 2018, Chap. 18, pp. 375–398.

[5] eSites Network, "Everything you wanted to know about Nickel and Nickel Alloys," https://www.nickel-alloys.net/article/commercially-pure-, ???? Accessed: 2024-2-25.

[6] Powers, L., "Stainless steel characteristics: A pocket guide," https://eagletube.com/about-us/news/stainless-steel-characteristics/, Jun. 2019. Accessed: 2024-2-26.

[7] ESPI Metals, "Silver — Sterling Technical Data," https://www.espimetals.com/index.php/technical-data/81-, n.d. Accessed: 2024-02-26.

[8] Chandler, D. L., "How to remove dust on solar panels without using water, improving overall efficiency," https://energy.mit.edu/news/how-to-remove-dust-on-solar-panels-without-using-water-improving-overall-efficiency/, Jul 21 2022. Accessed: 2026-02-27.